NASA TECHNICAL NOTE

NASA TN D-4040

DYNAMIC RESPONSE OF GASEOUS-HYDROGEN FLOW SYSTEM AND ITS APPLICATION TO HIGH-FREQUENCY COMBUSTION INSTABILITY

by Charles E. Feiler and Marcus F. Heidmann

Lewis Research Center
Cleveland, Ohio

NATIONAL AERONAUTICS AND SPACE ADMINISTRATION • WASHINGTON, D. C. • JUNE 1967

NASA TN D-4040

DYNAMIC RESPONSE OF GASEOUS-HYDROGEN FLOW SYSTEM AND ITS APPLICATION TO HIGH-FREQUENCY COMBUSTION INSTABILITY

By Charles E. Feiler and Marcus F. Heidmann

Lewis Research Center
Cleveland, Ohio

NATIONAL AERONAUTICS AND SPACE ADMINISTRATION

For sale by the Clearinghouse for Federal Scientific and Technical Information
Springfield, Virginia 22151 – CFSTI price $3.00

DYNAMIC RESPONSE OF GASEOUS-HYDROGEN FLOW SYSTEM AND ITS APPLICATION TO HIGH-FREQUENCY COMBUSTION INSTABILITY

by Charles E. Feiler and Marcus F. Heidmann

Lewis Research Center

SUMMARY

The dynamic response characteristics of a lumped-element model of a gaseous-hydrogen injector were determined. The investigation was conducted to determine whether coupling between hydrogen flow oscillations and chamber pressure oscillations could be large enough to provide a mechanism for driving high-frequency combustion instability. The model was derived in terms of the injector design variables and was evaluated for three engines of different scales. The results are presented to show the effect of hydrogen density (temperature) on the coupling, since this parameter is useful in determining stability limits experimentally. A comparison of predicted and experimental stability limits was made which showed general agreement between experiment and theory. Such flow system coupling has been known to be of importance in low-frequency instability for some time. The present results show that, for gaseous flow systems, flow system coupling is an important factor in causing high-frequency instability also.

INTRODUCTION

An analysis was made of the dynamic response of the flow in a gaseous-hydrogen injector to determine whether the flow could couple with high-frequency chamber pressure oscillations to drive high-frequency combustion instability. While such coupling has been demonstrated for liquid flow at a low frequency, it apparently has not been considered for gaseous flow at a high frequency.

In this analysis, the hydrogen injector was modeled as a lumped-element system. Also, the equations describing the systems were linearized by a perturbation technique. Although the injector probably cannot be precisely described by a lumped-element system, the results should serve to illustrate the importance of flow system coupling on instability.

The analysis is presented in terms of the injector and engine parameters that are

ordinarily varied in engineering design. It has been examined over a range of parameters by considering three engines of widely differing scales. The results are presented to show the effect of increasing hydrogen density (decreasing hydrogen temperature) on the coupling between oscillations in hydrogen flow and chamber pressure. Hydrogen density was chosen for the independent parameter to facilitate comparison of the results with the experimental data of reference 1. These experimental studies (ref. 1) employed a hydrogen temperature-ramping technique in which the hydrogen injection temperature was gradually decreased until instability occurred. This transition temperature was then used to rate the various injector schemes and engine designs; the lower the transition temperature, the more stable the system was considered to be. The comparison of these data with the present analytical results gives some indication of the significance of the analysis in a qualitative manner.

SYMBOLS

A	cross-sectional area, in.^{2} (cm^2)
C	capacitance term (eq. 19(a)), sec
g	gravitational constant, 32.174 lb mass-ft/lb force-sec^2 (1 kg - m/N - sec^2)
I	inertia term (eq. 19(a)), sec
L	hydrogen annulus length, in. (cm)
$(L/A)_{eff}$	effective value of (L/A_1), in.$^{-1}$ (cm^{-1})
M	hydrogen mass in dome, lb mass(kg)
N	response factor (eq. (1) or (2))
O/F	oxidant-fuel mixture ratio
P_c	chamber pressure, lb force/in.^{2}(N/m^2)
P_d	dome pressure, lb force/in.^{2}(N/m^2)
P_1	annulus entrance pressure, lb force/in.^{2}(N/m^2)
P_2	orifice entrance pressure, lb force/in.^{2}(N/m^2)
R_1, R_2	pressure-ratio functions, (eq. (22))
s	Laplace operator
T	temperature, $^\circ$R ($^\circ$K)
t	time, sec
U	velocity, ft/sec (m/sec)

V	dome volume, in.^{3} (cm^3)
W	flow rate through injector, lb mass/sec (kg/sec)
W_b	flow rate of burned hydrogen gases, lb mass/sec (kg/sec)
W_{in}	dome inlet flow rate, lb mass/sec (kg/sec)
W_t	total flow rate, hydrogen and oxygen, lb mass/sec (kg/sec)
γ	specific-heat ratio
θ	phase angle between P_c' and W'
ρ	hydrogen density, lb mass/ft^3 (kg/m^3)
τ_b	time delay constant for burning, sec
ψ	reactance, eq. (26)
ω	frequency, rad/sec

Subscripts:

lox	liquid oxygen
max	peak amplitude of sine wave
noz	nozzle
1	hydrogen annulus
2	hydrogen orifice

Superscripts:

$\bar{}$	average value
$'$	perturbation quantity, $(x - \bar{x})/x$

ANALYSIS

Conceptual Philosophy

The analysis was conducted to determine the extent to which the hydrogen flow could couple with chamber pressure oscillations to drive them. The analysis differs from the usual frequency-response analysis in that the frequency and oscillation mode characteristics were fixed by engine geometry, and the effects of other parameters on the coupling were examined. The result of the analysis is a response factor N that gives the real part of the hydrogen-flow-rate oscillation in phase with the chamber pressure oscillation. The response factor as derived in reference 2 for sinusoidal oscillations is

$$N = \frac{(W'_{max})}{(P'_{c,\,max})} \cos\theta \tag{1}$$

where $P'_c = (P'_{c,\,max})\sin\omega t$ and $W' = W'_{max}\sin(\omega t + \theta)$.

Before the response factor for the hydrogen flow is calculated, a brief discussion of its significance and use is presented. A system with a positive response factor (in-phase coupling) should provide a driving source, and a system with a negative response factor (out-of-phase coupling) should provide damping. In this isolated system, neutral stability should correspond to a response factor equal to zero. In a rocket engine, stability is controlled by several processes that act simultaneously and may be sources of either driving or damping. In the real case of interest then, stability would occur if each response factor were zero; however, a more realistic criterion would seem to require only that the sum of the response factors be zero or that the gains of the entire system be equal to the losses. This criterion holds for a volume in which the pressure oscillates uniformally. It is also applicable to a transverse mode in a rocket combustor with uniform injection and a uniformally distributed nozzle. The following expression defining stability in terms of the response factor and representing the foregoing criterion was assumed:

$$\sum N = \frac{\overline{W_t}}{\overline{W_t}} N_{noz} + \frac{\overline{W_{lox}}}{\overline{W_t}} N_{lox} + \frac{\overline{W_{H_2}}}{\overline{W_t}} N_{H_2} = 0 \tag{2}$$

where the response factors N_{noz}, N_{lox}, and N_{H_2} are for the nozzle flow, the oxygen vaporization or combustion, and hydrogen flow, respectively. In the summation, each response factor was weighted by the fraction of the mean total weight flow involved in the particular process. To use this relation, an evaluation of the oxygen and nozzle response factors is needed. For oxygen, the peak linear response factor N_{lox} of 0.55 from reference 2 was used as an approximation.

For the nozzle response factor, the simplest assumption was to consider the nozzle as a purely resistive element and to neglect velocity effects. From the continuity relation,

$$W = -\rho A U \tag{3}$$

which, in perturbation form, gives

$$W' = -\rho' = -\frac{P'}{\gamma} \tag{4}$$

where $P = \rho^{\gamma}$ and $P' = \gamma\rho'$.

According to equation (1) the nozzle response factor for this model is

$$N_{noz} = -\frac{1}{\gamma} = -0.833 \qquad \text{for } \gamma = 1.2$$

An approximation to the value of the hydrogen response factor at the stability limit becomes possible through the use of equation (2) and these values of the nozzle and oxygen response factors.

Hydrogen System Model

In figure 1, a single coaxial injector element of the hydrogen flow system is shown. The coaxial injector type is the predominant choice in practice for the hydrogen-oxygen propellant combination. It consists of an annular orifice (area A_2) connected by an annular passage (area A_1 and length L) to a supply dome or cavity (volume V). It is assumed that the dome is supplied at a constant flow rate W_{in}. A transfer function for these elements that dynamically relates the flow rate to the chamber pressure is first derived; from this the response factor can be derived directly. As stated earlier, the equations in perturbation form are linearized.

Supply dome (capacitance). - For the fluid in the dome, a mass balance gives

$$\frac{dM}{dt} = W_{in} - W \tag{5}$$

Since W_{in} is a constant and $M = \rho V$, in perturbation form equation (5) becomes

$$\frac{\overline{\rho}_d V}{\overline{W}} s\rho' = -W' \tag{6}$$

where s is the Laplace operator. Throughout this development, the adiabatic relation between pressure and density is used. In perturbation form this relation is

$$P' = \gamma\rho' \qquad \text{where } \gamma = \gamma(T) \tag{7}$$

Substitution of equation (7) into (6) yields

$$\frac{\overline{\rho}}{\gamma}\frac{V}{\overline{W}}\,sP'_d = -W' \tag{8}$$

Annular entrance loss (resistance). - The flow from the dome into the annulus is represented by a resistive entrance loss for which the orifice flow relation is assumed:

$$W = KA_1\sqrt{(P_d - P_1)\rho g} \tag{9}$$

With the aid of equation (7), in perturbation form,

$$W' = \frac{1}{2}\left[\frac{\overline{P}_d}{\Delta P_1}P'_d + \left(\frac{1}{\gamma} - \frac{\overline{P}_1}{\Delta P_1}\right)P'_1\right] \qquad \text{where } \Delta P_1 = \overline{P}_d - \overline{P}_1 \tag{10}$$

Annulus flow loss (inductance). - The flow in the annulus is assumed to be of slug form. The associated inertia is obtained from the momentum and continuity relations with the assumption of an average density and velocity over the length of the annulus.

$$P_1 - P_2 = \frac{L}{gA_1}\frac{dW}{dt} \tag{11}$$

or

$$\overline{P}_1P'_1 - \overline{P}_2P'_2 = \frac{\overline{W}L}{gA_1}sW' \tag{12}$$

If it is assumed that $\overline{P}_1 = \overline{P}_2$, then

$$P'_1 - P'_2 = \frac{\overline{W}L}{g\overline{P}_2A_1}sW' \tag{13}$$

Final orifice (resistance). The final orifice yields

$$W = KA_2\sqrt{(P_2 - P_c)\rho g} \tag{14}$$

or

$$W' = \frac{1}{2}\left[\frac{\overline{P}_2}{\Delta P_2} P_2' + \left(\frac{1}{\gamma} - \frac{\overline{P}_c}{\Delta P_2}\right) P_c'\right] \qquad \text{where } \Delta P_2 = \overline{P}_2 - \overline{P}_c \tag{15}$$

Burning process. - In addition to the relations presented thus far, it is assumed that before the hydrogen can contribute to the chamber pressure it must, in some way, by diffusion and mixing and reaction, be brought to the chamber temperature. This step is represented simply by a delay time. Thus,

$$W_b(t) = W(t - \tau_b) \tag{16}$$

and

$$W_b' = W' e^{-\tau_b s} \tag{17}$$

The perturbation expressions (eqs. (8), (10), (13), (15), and (17)) may be combined to give the transfer function

$$\frac{W_b'}{P_c'} = - \frac{\left(\frac{\overline{P}_c}{\Delta P_2} - \frac{1}{\gamma}\right)\left(\frac{\overline{P}_2}{\Delta P_1} - \frac{1}{\gamma}\right)\left(\frac{\Delta P_2}{\overline{P}_2}\right)\left(\frac{\Delta P_1}{\overline{P}_d}\right) C s e^{-\tau_b s}}{1 + 2\frac{\Delta P_1}{\overline{P}_d}\left[1 + \frac{\Delta P_2}{\overline{P}_2}\left(\frac{\overline{P}_2}{\Delta P_1} - \frac{1}{\gamma}\right)\right] Cs + \frac{\Delta P_1}{\overline{P}_d}\left(\frac{\overline{P}_2}{\Delta P_1} - \frac{1}{\gamma}\right) CIs^2} \tag{18}$$

where

$$\left.\begin{aligned} C &\equiv \frac{\overline{\rho} V}{\gamma \overline{W}} \\ \text{and} \\ I &\equiv \frac{\overline{W}\left(\frac{L}{A_1}\right)}{g\overline{P}_2} \end{aligned}\right\} \tag{19}$$

Following the procedure of reference 2, the response factor N given by equation (1) is

$$N = \left(\frac{W'_{b,\max}}{P'_{c,\max}}\right)\cos\theta \tag{20}$$

where

$$\frac{W'_{b,\max}}{P'_{c,\max}} = -\frac{\left(\frac{\overline{P}_c}{\Delta P_2} - \frac{1}{\gamma}\right)\left(\frac{\overline{P}_2}{\Delta P_1} - \frac{1}{\gamma}\right)\left(\frac{\Delta P_2}{\overline{P}_2}\right)\left(\frac{\Delta P_1}{\overline{P}_d}\right)C\omega}{\left(\left[1 - \frac{\Delta P_1}{\overline{P}_d}\left(\frac{\overline{P}_2}{\Delta P_1} - \frac{1}{\gamma}\right)CI\omega^2\right]^2 + \left\{2\frac{\Delta P_1}{\overline{P}_d}\left[1 + \frac{\Delta P_2}{\overline{P}_2}\left(\frac{\overline{P}_2}{\Delta P_1} - \frac{1}{\gamma}\right)\right]C\omega\right\}^2\right)^{1/2}} \tag{21}$$

and

$$\theta = \frac{\pi}{2} - \omega\tau_b - \tan^{-1}\frac{2\frac{\Delta P_1}{\overline{P}_d}\left[1 + \frac{\Delta P_2}{\overline{P}_2}\left(\frac{\overline{P}_2}{\Delta P_1} - \frac{1}{\gamma}\right)\right]C\omega}{1 - \frac{\Delta P_1}{\overline{P}_d}\left(\frac{\overline{P}_2}{\Delta P_1} - \frac{1}{\gamma}\right)CI\omega^2} \tag{22}$$

By defining two dimensionless parameters,

$$R_1 \equiv \frac{\overline{P}_d}{\overline{P}_2 - \frac{\Delta P_1}{\gamma}}$$

and

$$R_2 \equiv \frac{\overline{P}_2}{\overline{P}_c - \frac{\Delta P_2}{\gamma}} \tag{23}$$

equations (21) and (22) may be more simply expressed:

$$\frac{W'_{b,\max}}{P'_{c,\max}} = -\frac{1}{R_2\left\{\left(\frac{R_1}{C\omega} - I\omega\right)^2 + \left[2\left(\frac{R_1\,\Delta P_1}{\overline{P}_d} + \frac{\Delta P_2}{\overline{P}_2}\right)\right]^2\right\}^{1/2}} \tag{24}$$

$$\theta = \frac{\pi}{2} - \omega\tau_b - \tan^{-1}\frac{2\left(\frac{R_1\,\Delta P_1}{\overline{P}_d} + \frac{\Delta P_2}{\overline{P}_2}\right)}{\frac{R_1}{C\omega} - I\omega} \tag{25}$$

A final simplification is made by defining a reactance ψ where

$$\psi = \frac{\frac{R_1}{C\omega} - I\omega}{2\left(\frac{R_1\,\Delta P_1}{\overline{P}_d} + \frac{\Delta P_2}{\overline{P}_2}\right)} \tag{26}$$

This results in the following modified response factor:

$$N\left[2R_2\left(\frac{R_1\,\Delta P_1}{\overline{P}_d} + \frac{\Delta P_2}{\overline{P}_2}\right)\right] = -\frac{1}{\sqrt{\psi^2 + 1}}\cos\left(\frac{\pi}{2} - \omega\tau_b - \tan^{-1}\frac{1}{\psi}\right) \tag{27}$$

ANALYTICAL RESULTS

General Behavior of Model

Equation (27) represents analytically the dynamic response of the flow for the injector element of figure 1. This equation is plotted in figure 2 for both positive and negative values of ψ and for values of $\omega\tau_b$ from 0 to π radians. In this figure, the response of the flow system alone is given by the curve for $\omega\tau_b = 0$. For $\omega\tau_b = 0$, the hydrogen flow system tends to be a damping process, as shown by the negative response factor, because the flow oscillations are out of phase with chamber pressure oscillations. At large ψ, either positive or negative, the response factor approaches zero because the flow no longer responds to pressure oscillations and because the phase angle approaches 90°. At the unique point $\psi = 0$, the response curve attains its maximum value (negative).

At this point, the system is, in a sense, tuned and the flow oscillations are exactly 180° out of phase with pressure oscillations. The value of the response factor then depends only on the resistive pressure drop terms.

At $\omega\tau_b = 0$, W' and P_c' are 180° out of phase as just stated. As $\omega\tau_b$ is increased from 0 to $\pi/2$, the response factor becomes less negative and is zero at $\omega\tau_b = \pi/2$, where W' and P_c' are phase displaced by 90°. As $\omega\tau_b$ is increased from $\pi/2$ to π, the response factor becomes more positive and attains a maximum at $\omega\tau_b = \pi$. At this point, W' and P_c' are exactly in phase. The further increase of $\omega\tau_b$ from π to 2π is not shown in figure 2, but it results in the response factor decreasing to its value at $\omega\tau_b = 0$. A similar behavior occurs at other values of ψ, but it is more obscure because of the effect of ψ on both $W'_{,max}/P'_{c,max}$ and θ. The limiting curve of the response factor is given by the dashed line. This curve is obtained at each value of ψ by adjusting $\omega\tau_b$ so that $\theta = 0$.

Parametric Study

The response factor was calculated for three engines to show the effect of the different parameters. These were the engine of reference 1, which is similar to the RL-10 and engines A and B, about the size of the M-1 and J-2, respectively. The three engines differ greatly in scale, as shown by the parameters listed in table I. Each of the parameters A_2, V, and L/A was evaluated at one-half and twice the value listed in table I to show the sensitivity of the response factor to the parameters.

For the inertia term, an effective value of (L/A_1), $(L/A)_{eff}$ composed of the sum of two contributions, was used. The contributions considered were those from the final orifice and the annular passage. No correction for effective length was made in this evaluation. The individual injector elements were assumed to behave as isolated units. The volume for an individual element was approximated as the ratio of the volume of the dome to the number of elements. Since the calculations were made with the use of total hydrogen flow rates and injection areas, the total dome volume could be used in the numerical procedure.

The time delay τ_b was unknown but its use is justified as a simple representation of the history of the hydrogen gas between injection and combustion. For a typical hydrogen injection velocity of 500 feet per second (152 m/sec) and a τ_b of 0.0001 second, the events represented would have to occur in a space of 0.6 inch (1.52 cm). This distance approximates the standoff distance that has been observed for the flame; however, the significance of τ_b may be more complex or even unrelated to such a simple concept. The value of τ_b (0.00009 sec) used for the engine of reference 1 more closely represented the data, as is shown later.

TABLE I. - CALCULATION PARAMETERS

Parameter	Engine		
	Reference 1	B	A
Chamber pressure, P_c, lb force/in.^{2} (N/m^2)	300 (20.7×10^5)	680 (46.9×10^{-5})	1000 (69.0×10^5)
Total flow rate, W_T, lb mass/sec (kg/sec)	65 (29.5)	463 (210)	3420 (1550)
Frequency, ω, rad/sec	21 350	11 840	5340
Oxidant-fuel ratio, O/F	5.5	5.5	5.5
Hydrogen orifice area, A_2, in.^{2} (cm^2)	4.62 (29.8)	25.7 (166)	69 (445)
Dome volume, V, in.^{3} (cm^3)	46.0 (754)	274 (4490)	1690 (27 700)
Hydrogen annulus length to area ratio, (L/A)eff, in.$^{-1}$ (cm^{-1})	0.0677 (0.0267)	0.0102 (0.0040)	0.0046 (0.0018)
Hydrogen annulus area, A_1, in.^{2} (cm^2)	9.12 (58.8)	68.2 (440)	205.5 (1325)
Time delay constant for burning, τ_b, sec	0.00009	0.0001	0.0001
Hydrogen density, ρ, lb/ft^3 (kg/m^3)	0.1 to 4.04 (1.60 to 6.47)	0.1 to 4.04 (1.60 to 16.47)	0.1 to 4.04 (1.60 to 6.47)
Temperature, T, $^\circ$R ($^\circ$K)	[a]~645 to ~50 (358 to 27.8)	[b]~1400 to ~55 (778 to 30.6)	[c]~2150 to ~60 (1195 to 33.3)

[a]At 20 atm (20.3×10^5 N/m^2).
[b]At 43 atm (43.6×10^5 N/m^2).
[c]At 70 atm (71×10^5 N/m^2).

Since the Mach number of the flow was low, one further approximation that was made was the use of a constant average density in calculating the mean values of the pressure drop terms ΔP_1 and ΔP_2. A discharge coefficient of 1, was also assumed.

In figure 3, the variation of the response factor with hydrogen injection density is shown with the injector design parameters as variables. The effect of ramping the hydrogen temperature is readily seen. Figure 3(a) shows the oxidant-fuel ratio O/F as a variable; increasing O/F tends to increase the magnitude of the response factor. Figure 3(b) shows a similar result with the final orifice area A_2 as a variable. The major effect is upon the resistive terms. Increasing either O/F or A_2 at a constant total weight flow W_t causes a reduction in the pressure drop ΔP_2 across the orifice A_2. As a result, the coupling between W' and P'_c is greater as is the absolute value of the response factor. For the A and B engines, this coupling was out of phase while for

the reference 1 engine it was in phase.

Figures 3(c) and (d) show the effect of V and $(L/A)_{eff}$, respectively. The effect of increasing either term is qualitatively the same, since an increase in either results in a change in the value of ψ to more negative values. Neither V nor $(L/A)_{eff}$ affects the resistive terms. The result is that the peak or any point on the $\dot{\psi}$ curve (fig. 2) occurs at a different density and at a different resistance, which shifts the response factor curves so that similar points, such as the minimums and zero response factor, occur at different densities. In figures 3(a) and (b), where the primary effect was on the resistive terms, these corresponding points occur at about the same density for a particular engine.

The general effect of increasing density, as shown by all the curves in figure 3, was to increase the absolute value of the response factor. Increasing the density has two primary effects: first is that of lowering the resistance, or pressure drop, which results in a greater coupling, and second is that of shifting the ψ toward more negative values. The major part of the effect on ψ occurs by the increase in the capacitive term C, which is directly proportional to the density. The inertia term I is not strongly influenced by density.

One other general point can be made about the nature of the curves of figure 3. The density at which the response factor is zero occurs when the total angle θ is $\pi/2$. This density differs among engines because the resonant frequency and the ψ values differ.

The parameters that were evaluated are related to injector design and to the scale of the engine. Other parameters such as contraction ratio would also influence the response factor by affecting the chamber pressure, weight-flow rate, or resonant frequency. These parameters have not been included as a part of this study.

The results of the analysis show an appreciable coupling of the hydrogen flow oscillations with the chamber pressure oscillations. Hydrogen density is shown to be an important factor in the coupling. For a given engine, the variation of selected injector parameters over a range of 4 to 1 did not change the basic character of the response factor for that engine. This basic character appears to be determined by the scale of the engine, in that one of the important parameters was the resonant frequency. For a constant time delay, as was assumed, the phase angle θ is strongly influenced by the contribution of $\omega\tau_b$ to θ. This influence, in turn, determines whether the basically out-of-phase coupling between flow and pressure oscillations can be shifted to become in phase.

COMPARISON OF EXPERIMENT AND ANALYSIS

The engine of reference 1 offers an opportunity for comparing experimental and

analytical results. The hydrogen-temperature stability limit of this engine was experimentally determined as a function of O/F for three hydrogen injection areas with the same oxygen injector. Figure 4 shows the response-factor - density curves calculated for this engine over a range of O/F values and for three orifice areas A_2. The response factor increased with density for this particular engine. As a result, decreasing hydrogen temperature (increasing density) should cause the engine to become unstable. The value of the hydrogen response factor at the stability limit was calculated by using equation (2) and the values of nozzle and oxygen-system response factors given previously. From figure 4, the density corresponding to the hydrogen response factor may be obtained.

In figure 5, the stability limit data of reference 1 are replotted to show hydrogen density rather than temperature as a function of O/F. The data show the hydrogen density separating stable and unstable operation. The curves are predicted from the analysis. The curve $A_2 = 4.62$ square inches (29.8 sq cm) was obtained by selecting a value of the time delay τ_b that reasonably approximated the data. For this purpose, τ_b was 0.00009 second, and this value was used for the remaining injectors. With this procedure, the analysis overpredicted the injector of $A_2 = 1.41$ square inches (9.1 sq cm) by about 50 percent. The injector with $A_2 = 0.77$ square inch (5.0 sq cm) was essentially stable at the lowest density attainable in the experiment. The calculation for this injector also indicated that it was stable to a density greater than that attainable.

From this comparison with the data of reference 1, it can be seen that, while agreement was not perfect, the trends with both O/F and the hydrogen injection area were predicted. Better agreement could probably have been obtained by allowing the time delay to vary with the hydrogen injection area; however, too little is known about the time delay to justify its variation. In making the comparison, it was also assumed that changing the hydrogen injection area did not influence the oxygen response factor. Relaxing this assumption might also improve the agreement. The important conclusion, however, can still be made: the hydrogen flow is sufficiently sensitive that the coupling between hydrogen flow oscillations and chamber pressure oscillations can drive instability.

Similar experimental data were not available for other engines. The present analysis indicates that engine A (M-1 size) should be a stable configuration with regard to the hydrogen flow system, as shown in figure 3(a), where the response factor is generally negative. For engine B (J-2 size), figure 3(a) shows that the response factor increases rapidly at a density greater than 2.5 pounds per cubic foot (40 kg/cu m). At the pressure level of the B engine, this density occurs at about 60° R (33° K). As more data become available, they may provide insight into the importance of various parameters in the model that has been presented and thus permit a more realistic model to be derived. This method of analysis also predicts qualitatively the increased stability (lower hydrogen temperature or higher density) of large oxygen jets reported in reference 1.

In this case, a lower value of oxygen response factor for large jets and drops as predicted in reference 2 is used in the summation of response factors (eq. (2)). Such a trade off between oxygen and hydrogen response factors gives higher density (lower temperature) stability limits for larger diameter oxygen jets.

SUMMARY OF RESULTS

A lumped-element analysis of the response of a hydrogen-feed system to high-frequency chamber-pressure oscillations was made. The results may be summarized as follows:

1. For the injector model assumed, there was sufficient coupling between flow and pressure oscillations for this coupling to be an important factor in instability in gaseous-hydrogen systems.

2. Hydrogen density, an important variable in experimental studies, was also shown to be important in the analysis. Coupling of the flow and pressure oscillations increased with density.

3. Although appreciable coupling of the flow system to pressure oscillations was found, it was basically an out-of-phase coupling. The representation of the combustion process by a simple delay time concept changed the coupling from out of phase to in phase or from damping to driving.

4. A general agreement in trend between available experimental data and analytical predictions was found.

Lewis Research Center,
National Aeronautics and Space Administration,
Cleveland, Ohio, April 11, 1967,
128-31-06-02-22.

REFERENCES

1. Wanheinen, John P.; Parish, Harold C.; and Conrad, E. William: Effect of Propellant Injection Velocity on Screech in a 20 000-Pound Hydrogen-Oxygen Rocket Engine. NASA TN D-3373, 1966.

2. Heidmann, Marcus F.; and Wieber, Paul R.: An Analysis of the Frequency Response Characteristics of Propellant Vaporization. Paper No. 66-604, AIAA, June 1966.

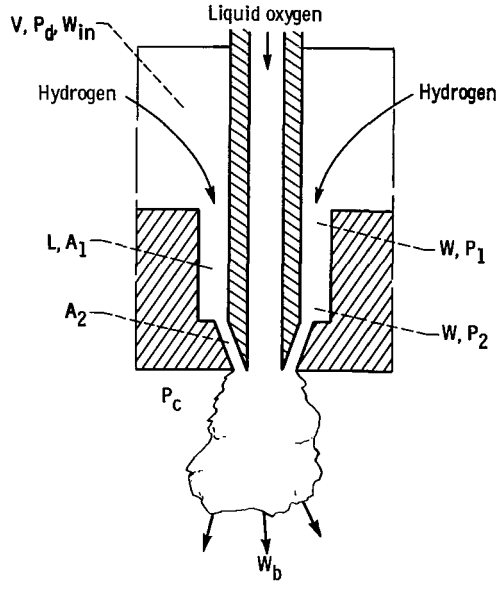

Figure 1. - Hydrogen injector element.

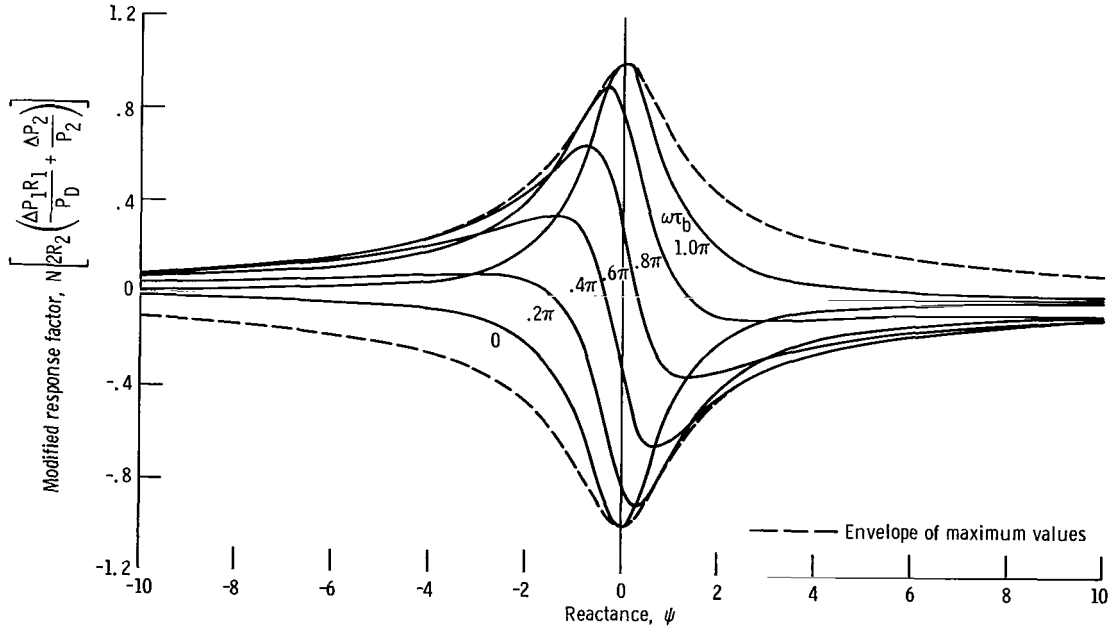

Figure 2. - Generalized response factor.

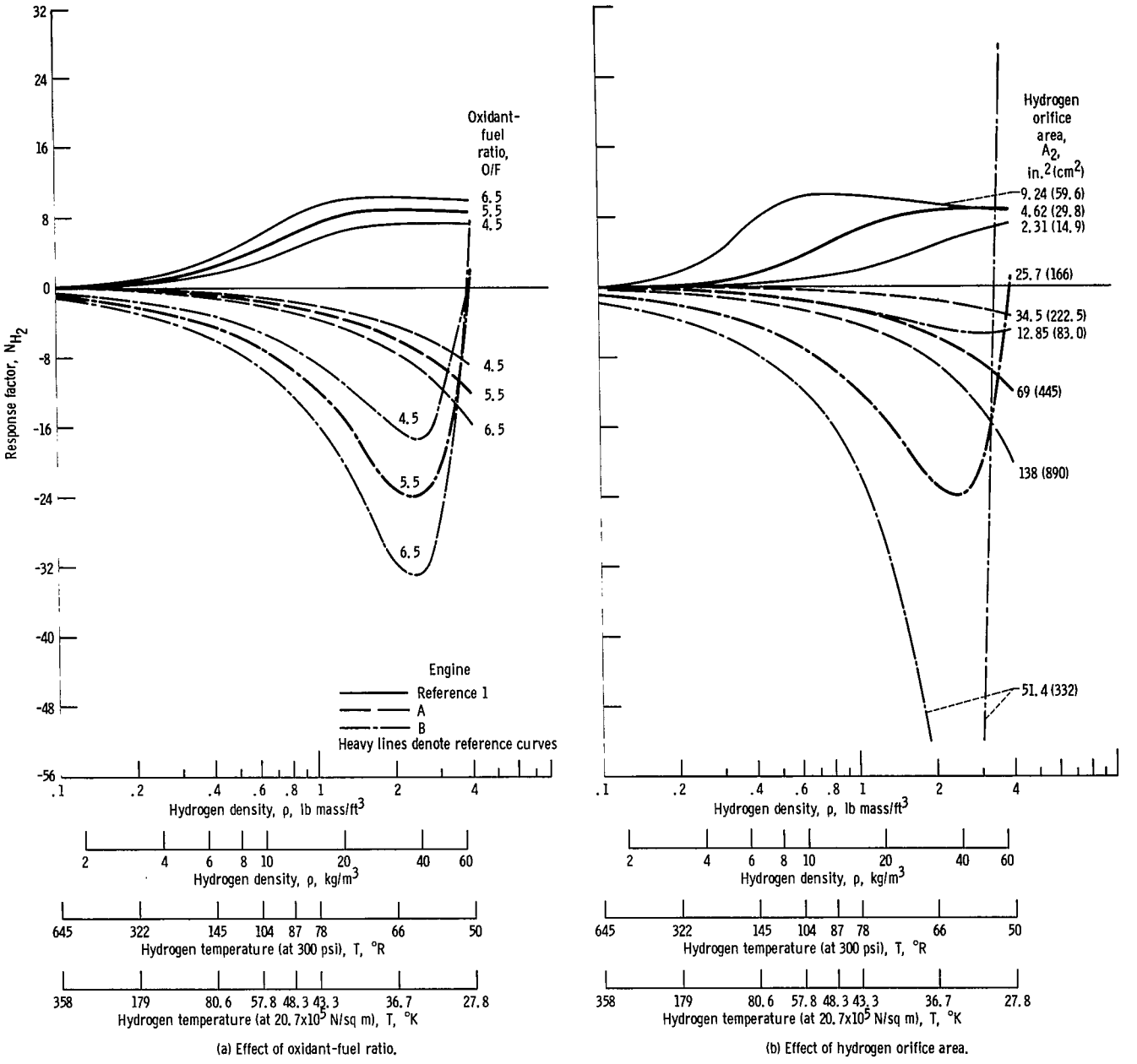

Figure 3. - Variation of response factor with hydrogen density.

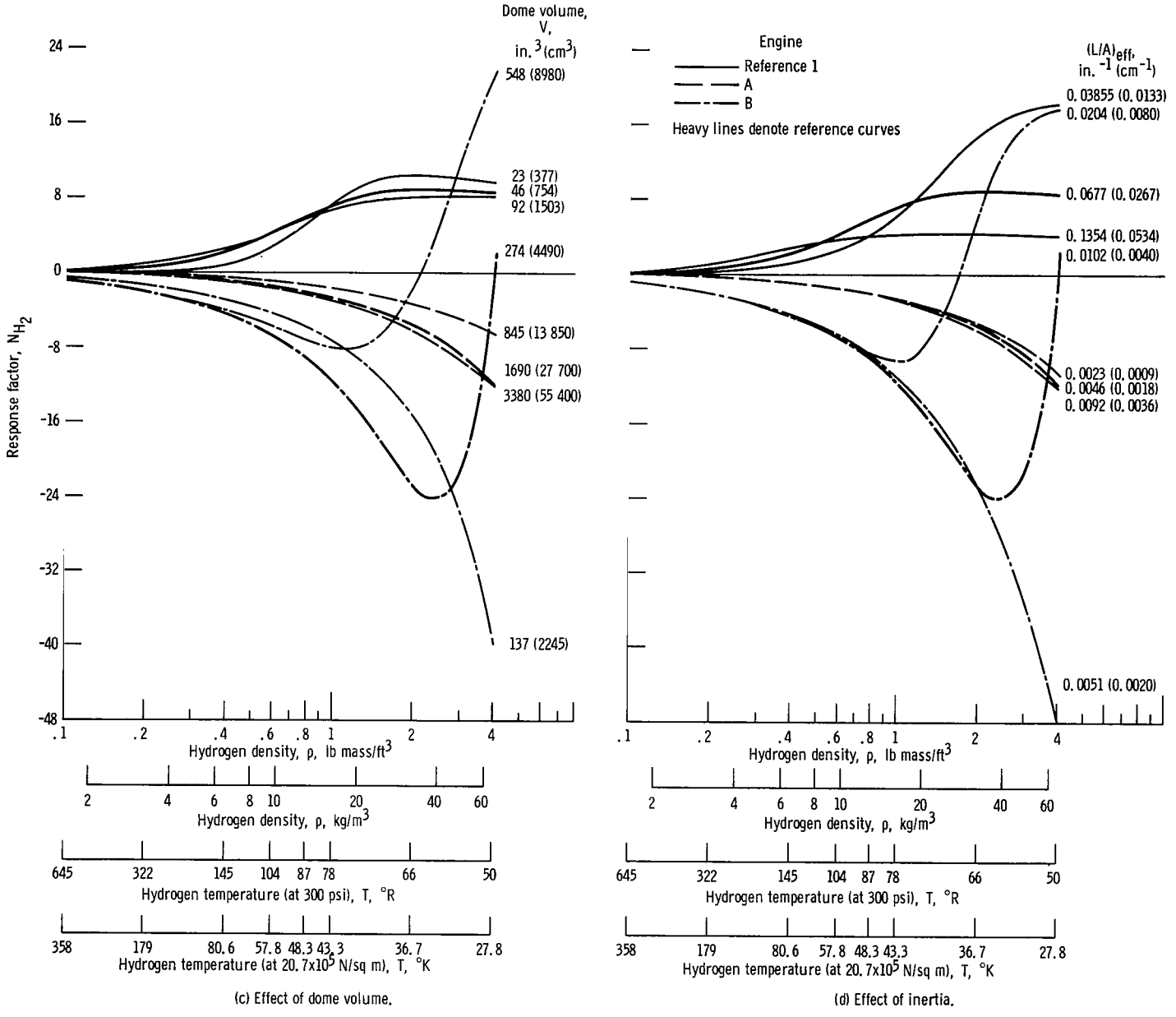

(c) Effect of dome volume.

(d) Effect of inertia.

Figure 3. - Concluded.

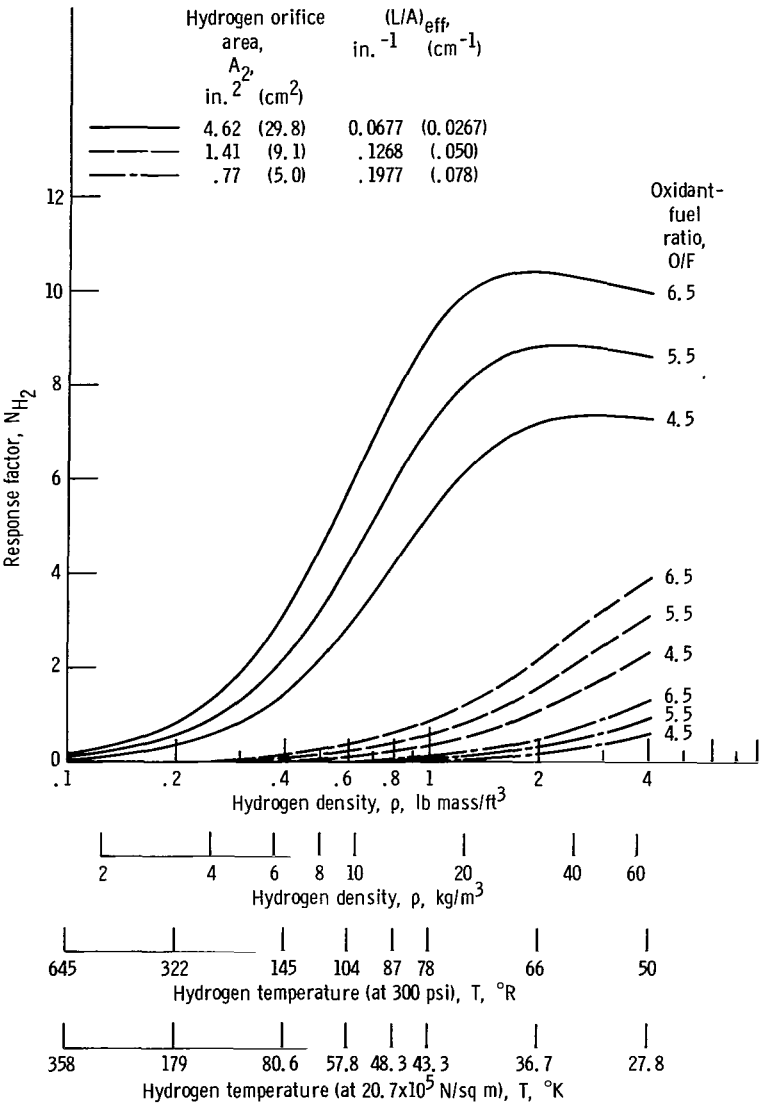

Figure 4. - Variation of response factor with hydrogen density for engine of reference 1.

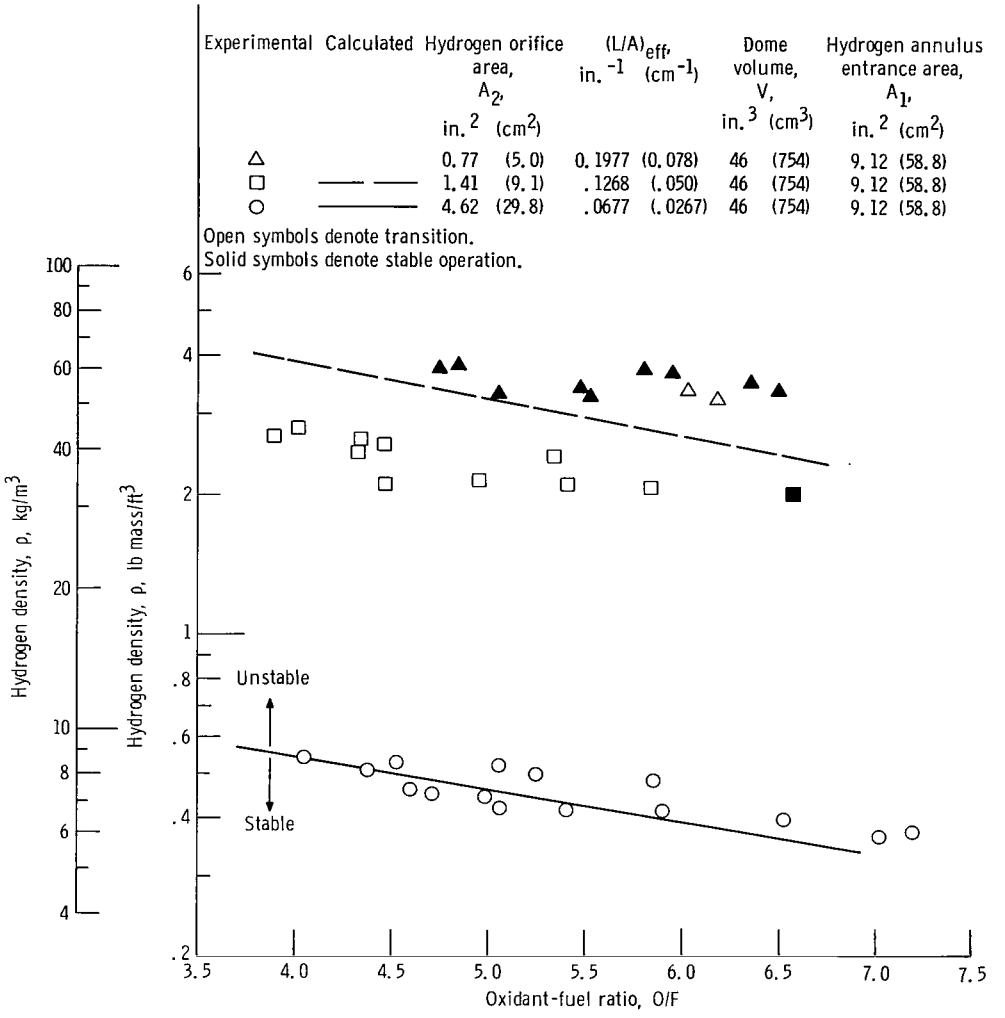

Figure 5. - Comparison of experimental and calculated hydrogen-density stability boundaries.

"The aeronautical and space activities of the United States shall be conducted so as to contribute . . . to the expansion of human knowledge of phenomena in the atmosphere and space. The Administration shall provide for the widest practicable and appropriate dissemination of information concerning its activities and the results thereof."

—NATIONAL AERONAUTICS AND SPACE ACT OF 1958

NASA SCIENTIFIC AND TECHNICAL PUBLICATIONS

TECHNICAL REPORTS: Scientific and technical information considered important, complete, and a lasting contribution to existing knowledge.

TECHNICAL NOTES: Information less broad in scope but nevertheless of importance as a contribution to existing knowledge.

TECHNICAL MEMORANDUMS: Information receiving limited distribution because of preliminary data, security classification, or other reasons.

CONTRACTOR REPORTS: Scientific and technical information generated under a NASA contract or grant and considered an important contribution to existing knowledge.

TECHNICAL TRANSLATIONS: Information published in a foreign language considered to merit NASA distribution in English.

SPECIAL PUBLICATIONS: Information derived from or of value to NASA activities. Publications include conference proceedings, monographs, data compilations, handbooks, sourcebooks, and special bibliographies.

TECHNOLOGY UTILIZATION PUBLICATIONS: Information on technology used by NASA that may be of particular interest in commercial and other non-aerospace applications. Publications include Tech Briefs, Technology Utilization Reports and Notes, and Technology Surveys.

Details on the availability of these publications may be obtained from:

SCIENTIFIC AND TECHNICAL INFORMATION DIVISION

NATIONAL AERONAUTICS AND SPACE ADMINISTRATION

Washington, D.C. 20546